

RARE B PHYSICS AT CLEO

Adam L. Lyon
University of Rochester, Rochester, NY 14627 USA
(For the CLEO Collaboration)

Abstract

I present selected preliminary rare B physics results from the CLEO experiment. An updated result on the inclusive $b \rightarrow s\gamma$ branching fraction is reported at $B(b \rightarrow s\gamma) = (3.15 \pm 0.35 \pm 0.32 \pm 0.26) \times 10^{-4}$, where the first uncertainty is statistical, the second is systematic, and the third for model dependence. I also describe a new analysis performed to search for CP asymmetry in $b \rightarrow s\gamma$ decays. We observe no such asymmetry and set conservative limits at $-0.09 < A < 0.42$. Finally, important to the search for CP violation in the Standard Model, the first observation of a hadronic $b \rightarrow u$ transition is reported in the mode $B^{\pm} \rightarrow \rho^0 \pi^{\pm}$ at a branching fraction of $(1.5 \pm 0.5 \pm 0.4) \times 10^{-5}$, where the uncertainties are statistical and systematic respectively.

1. Introduction

The effort of searching for rare processes involving B mesons at the CLEO experiment has reached almost industrial proportions. All of the analyses are important in searching for new physics and many are beginning to observe processes that will be useful in CP violation studies. Here, I present a small selection of CLEO's rare B program, namely determining the inclusive $b \rightarrow s\gamma$ branching fraction, a search for CP asymmetry in $b \rightarrow s\gamma$ decays, and the first observation of a hadronic $b \rightarrow u$ transition. Information regarding CLEO's other rare B analyses may be found elsewhere[1].

2. The CLEO Detector

Data for these analyses were taken with the CLEO detector at the Cornell Electron Storage Ring (CESR) with center of mass energy at the $\Upsilon(4S)$ resonance (10.58 GeV). Additional data were taken 60 MeV below the $\Upsilon(4S)$ (off-resonance) for continuum background subtraction. The CLEO detector[2] measures charged particles over 95% of 4π steradians with a system of cylindrical drift chambers. The barrel and endcap CsI calorimeters cover 98% of 4π , and the energy resolution for photons near 2.5 GeV in the central angular region ($|\cos \theta_\gamma| < 0.7$) is 2%. In 1995, a silicon vertex detector replaced the inner most tracking chamber, though it is not used in the analyses described here.

3. $b \rightarrow s\gamma$

Because flavor changing neutral currents are forbidden in the Standard Model, electroweak penguins such as $b \rightarrow s\gamma$ give a direct look at loop and box processes. The inclusive branching fraction for $b \rightarrow s\gamma$ is important for restricting physics beyond the Standard Model, and CLEO's 1995 published result[3] of $(2.32 \pm 0.57 \pm 0.35) \times 10^{-4}$ generated much theoretical interest[4]. The branching fraction result presented here is an improved measurement with 60% additional data and enhanced analysis techniques. The theoretical branching fraction prediction from the Standard Model has also improved, with a full next-to-leading-log calculation[5] of $(3.28 \pm 0.33) \times 10^{-4}$. We also introduce a new analysis: a search for CP asymmetry in $b \rightarrow s\gamma$.

3.1 $b \rightarrow s\gamma$ Branching Fraction

This analysis is discussed in detail elsewhere[6] and is briefly covered here. The signal for $b \rightarrow s\gamma$ is a photon from B meson decay with $2.1 < E_\gamma < 2.7$ GeV (the published analysis[3] used $2.2 < E_\gamma < 2.7$ GeV). The Fermi momentum of the b quark in the B meson and the momentum of the B meson in the lab frame (B mesons are produced from $\Upsilon(4S)$ decays with approximately 300 MeV/c of momentum at CESR) Doppler broadens the photon line shape. Calculations using a spectator model[7] indicate that 85-94% of the signal lies in the photon energy range.

To obtain a photon energy spectrum, we select hadronic events with a high energy calorimeter cluster in the central region ($|\cos \theta_\gamma| < 0.7$). We reject a cluster if, when paired with another calorimeter cluster in the event, it forms a combined $\gamma\gamma$ mass consistent with a π^0 or η . We also require the cluster shape be consistent with that of a single high energy photon.

A naïve approach to this analysis would be to measure the photon spectrum in on-resonance data and use the off-resonance data to subtract the continuum background. But the backgrounds from continuum with initial state radiation ($e^+e^- \rightarrow q\bar{q}\gamma$) (ISR) and from continuum processes ($e^+e^- \rightarrow q\bar{q}$) involving a high energy π^0 , η , or ω where one of the daughter photons is not detected dominate to such an extent that extraction of a signal is impossible. We therefore suppress the continuum background with two separate methods and subtract what remains with off-resonance data.

The first continuum suppression scheme[8] involves exploiting differences in the event shapes between signal ($B\bar{B}$) and continuum. While continuum events appear jetty and continuum with ISR appear jetty in the rest frame of the initial state photon, the signal events are spherical due to the other B meson decaying in the event. We characterize the event shape with eight variables[6], but since no one variable provides enough discriminating power, we combine them with a neural network into a single variable r . The

distribution of r tends towards -1 for continuum and ISR events and $+1$ for signal $b \rightarrow s\gamma$ events. This shape method is approximately 30% efficient for signal.

The other method of suppressing continuum and ISR events is a pseudo-reconstruction of the parent B meson involved in the $b \rightarrow s\gamma$ decay. We look for a charged or neutral kaon with up to four pions, one of which may be a π^0 , that emanate from a B meson. We try all combinations of kaons and pions with the constraints above and choose the one that minimizes a χ^2 that includes,

$$\chi_B^2 = \left(\frac{M - M_B}{\sigma_M} \right)^2 + \left(\frac{E - E_{beam}}{\sigma_E} \right)^2 \quad (1)$$

as well as contributions from particle identification such as dE/dx and π^0 and K_s^0 mass deviations. In Eq. (1), M is the beam constrained mass, $M = \sqrt{E_{beam}^2 - P^2}$ where P is the vector sum of particle momenta comprising the B meson candidate, M_B is the B mass ($5.279 \text{ GeV}/c^2$), E is the energy of the candidate B , and σ_M and σ_E are the resolutions on the beam constrained mass and the measured B energy respectively. Events that have a minimum $\chi_B^2 < 20$ are considered pseudo-reconstructed (*pseudo* is used because this method is only for continuum suppression, and we are not concerned that the parent B reconstruction be exactly correct). If the minimum $\chi_B^2 > 20$ or not one combination of kaons and pions were found in the event, then the shape analysis described above is used.

For events that are pseudo-reconstructed, we calculate the angle between the thrust axis of the inferred signal B meson and the thrust axis of the rest of the event ($\cos\theta_{||}$). Events that are in actuality continuum typically have $|\cos\theta_{||}|$ peaked at 1, while signal events have a flat $\cos\theta_{||}$ distribution. To get the most discriminating power, we combine χ_B^2 and $\cos\theta_{||}$ from the pseudo-reconstruction and r from the shape neural network into a new variable r_c using another neural network. As with r , the distribution of r_c tends towards $+1$ for signal events and -1 for continuum. While this combined method is 10% efficient for signal, it reduces the continuum background by an additional factor of four over the shape method alone.

We then weight each event according to its value of r_c if it is pseudo-reconstructed or r if not. The weighting scheme[6] is designed so that the weighted yield is equivalent to the event yield in the absence of continuum backgrounds. This procedure gives the smallest statistical uncertainty on this background subtracted yield. Note that there are non-continuum backgrounds discussed below, but these are small compared to continuum.

The continuum background remaining after the suppression efforts is determined from off resonance data. $B\bar{B}$ backgrounds are dominated by $b \rightarrow c$ (e.g. $B \rightarrow X\pi^0$ and $B \rightarrow X\eta$) though $b \rightarrow u$ and $b \rightarrow sg$ may have a small contribution. We estimate the $B\bar{B}$ backgrounds with Monte Carlo (MC), but correct the π^0 and η momenta spectra for any differences between data and MC. We obtain the momenta spectra from data by treating π^0 's and η 's as if they were photons and follow the same analysis procedure using weights described above. Thus, the MC is used only for the π^0 and η veto efficiencies and for any other small $B\bar{B}$ backgrounds not originating from missing a γ daughter from a π^0 or η .

The weighted yields from 3.1 fb^{-1} of on-resonance data plotted with respect to photon energy are shown in Fig. 1, with all of the backgrounds shown in (a) and the background subtracted weighted yield, which is the signal, shown in (b). 1.6 fb^{-1} of off-resonance data were used for the continuum subtraction. The expected spectrum for $b \rightarrow s\gamma$ from a spectator model is also shown in (b). In the region of interest ($2.1 < E_\gamma < 2.7 \text{ GeV}$) we measure 500.5 ± 7.4 on-resonance weighted events, 382.3 ± 7.0 scaled off-resonance weighted events, and estimate the $B\bar{B}$ background to be 53.4 weighted events (all uncertainties statistical). Applying the π^0 and η corrections to the $B\bar{B}$ estimate (0.19 ± 0.5 and 4.1 ± 1.1 weighted events respectively), we derive the weighted background subtracted yield of $92.2 \pm 10.3 \pm 6.5$, where the first uncertainty is statistical and the second is systematic.

For a typical sample of MC $b \rightarrow s\gamma$ events, approximately 50% pass all analysis requirements and of these, 40% are pseudo-reconstructed ($\chi_B^2 < 20$). But since we use weighted events for the signal yield, we

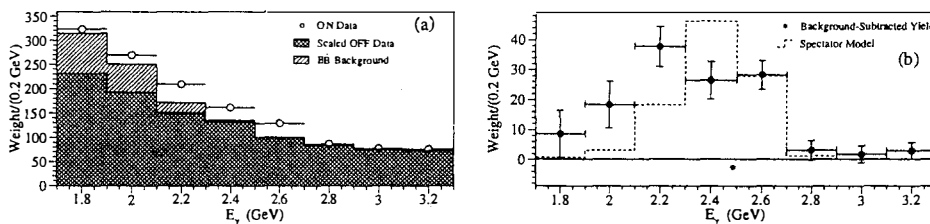


Figure 1. Photon energy spectra. (a) On-resonance data (points), luminosity scaled off-resonance data (double hatched), and $B\bar{B}$ background (single hatched). (b) Background-subtracted data (points) and Monte Carlo prediction of the shape of the $b \rightarrow s\gamma$ signal from a spectator model calculation ($\langle m_b \rangle = 4.88 \text{ GeV}/c^2$ and fermi momentum set at $250 \text{ MeV}/c$). Only statistical uncertainties are shown.

need a weighted efficiency; the sum of weights passing all requirements. Because of our definition of weights, the weighted efficiency tends to be smaller than the efficiencies stated above. To model the signal, we use the spectator model of Ali and Greub[7], which includes gluon bremsstrahlung and other higher order radiative effects. Details of MC production and parameters used are given in ref. 6. The weighed efficiency is $(4.43 \pm 0.29 \pm 0.22 \pm 0.03 \pm 0.31) \times 10^{-2}$, where the first uncertainty is due to spectator model inputs, the second due to recoil system hadronization, the third due to uncertainty in the production ratio of neutral and charged B meson pairs, and the last to detector modeling.

The weighted efficiency is combined with the background subtracted weighted yield to give the inclusive branching fraction of $b \rightarrow s\gamma$ as $(3.15 \pm 0.35 \pm 0.32 \pm 0.26) \times 10^{-4}$, where the uncertainties are statistical, systematic and for model dependence respectively. Our results are in agreement with the Standard Model prediction. Conservatively allowing for the systematic uncertainty, we find that the branching fraction must be between 2.0×10^{-4} and 4.5×10^{-4} (each limit at 95% CL).

3.2 $b \rightarrow s\gamma$ CP Asymmetry

The SM predicts no CP asymmetry in $b \rightarrow s\gamma$ decays, but some recent theoretical work[9] suggests that non-SM physics may significantly contribute to a CP asymmetry. Furthermore, if new physics has a weak phase difference near 90° with respect to the SM and the strong phase is non-zero, the new physics would only slightly alter the $b \rightarrow s\gamma$ inclusive branching ratio, but could produce a large effect in the asymmetry. Since we can reuse much of the machinery from the branching fraction measurement, a search for CP asymmetry is an obvious extension to the $b \rightarrow s\gamma$ analysis.

The pseudo-reconstruction procedure described above is used to tag the b quark flavor (b or \bar{b}), since it determines the particles decayed from the signal B meson. But since the pseudo-reconstruction was designed for continuum suppression, we must determine how often it reconstructs the b flavor correctly. If signal B meson decays to a neutral kaon and overall neutral pions (e.g. $B^0 \rightarrow K^0 \pi^+ \pi^-$), then we cannot determine the b flavor from pseudo-reconstruction. But for the majority of cases where the b flavor is determinable, it can be deduced by the charge of the kaon, or the sum pion charge if the kaon is neutral. From MC, we estimate the probability of reconstructing the *incorrect* b flavor when the b flavor is determinable to be $8.3 \pm 1.6\%$. The uncertainty is statistical combined with uncertainties derived from varying spectator model inputs to the MC and varying the ratio of charged to neutral B meson decays. We also take into account the probability of tagging the b flavor when it should be undeterminable and vice-versa, though these effects are small and will not be discussed further here.

The asymmetry we measure is $(N_1 - N_2)/(N_1 + N_2)$, where N_1 is the weighted yield tagged as b quarks from pseudo-reconstruction and determinable as such and N_2 is similarly the weighted yield tagged as \bar{b} . From the misreconstruction rates described above, we apply a multiplicative correction factor of 1.22 ± 0.04 to the asymmetry. In our misreconstruction determination, we assumed that the rate of mistagging a b as a \bar{b} was the same as mistagging a \bar{b} as a b . Initial studies lead us to apply a conservative addi-

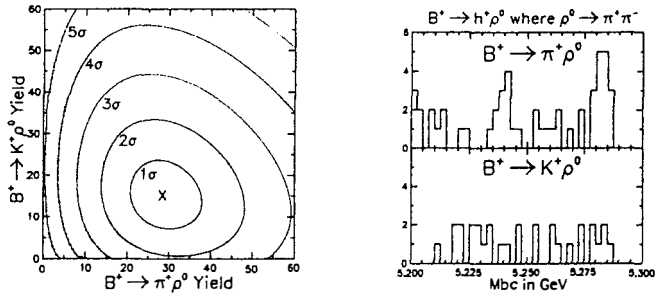


Figure 2. (a) Yield contours for $B^{\pm} \rightarrow \rho^0 \pi^{\pm}$ and $B^{\pm} \rightarrow \rho^0 K^{\pm}$ modes in the maximum likelihood fit. Note that the contours reflect statistical uncertainties only. (b) Projection of the beam constrained mass for $B^{\pm} \rightarrow \rho^0 \pi^{\pm}$ (top) and $B^{\pm} \rightarrow \rho^0 K^{\pm}$ (bottom). The $B^{\pm} \rightarrow \rho^0 \pi^{\pm}$ signal can be seen as the peak at the B meson mass in the top right plot.

tive systematic error on the asymmetry of 5% to account for unequal mistagging rates, though we observe no measurable asymmetry in the off-resonance data and other control samples.

Using the weighted yield from pseudo-reconstructed events with photons within $(2.2 < E_{\gamma} < 2.7 \text{ GeV})$, we observe 36.8 ± 5.2 weights reconstructed as b quarks and 28.4 ± 5.2 weights reconstructed as \bar{b} quarks (uncertainties are statistical only), leading to a raw asymmetry measurement of 0.13 ± 0.11 . Applying the correction factors, we obtain our preliminary CP asymmetry measurement in $b \rightarrow sy$ decays: $(0.16 \pm 0.14 \pm 0.05) \times (1.0 \pm 0.04)$, where the first number is the central value, the second is the statistical uncertainty, the third is the additive systematic described above, and the multiplicative factor is from the uncertainty on the mistagging rate correction. Within the uncertainties, we measure no CP asymmetry. From this result, we derive 90% confidence level limits on the CP asymmetry (A) of $-0.09 < A < 0.42$.

4. First Observation of $B^{\pm} \rightarrow \rho^0 \pi^{\pm}$

The study of charmless B decays involving $b \rightarrow u$ is important, because the contribution from tree processes is suppressed. Interference between tree and penguin processes may then result in CP violation. Here we briefly discuss CLEO's first observation of such a charmless B decay to $\rho^0 \pi^{\pm}$. See ref. 1 for additional information.

This analysis involves searching for the decay of a charged B meson to $h^{\pm} K^{\mp}$ and $h^{\pm} \rho^0$ (a pseudoscalar and a vector), where h is a pion or kaon. The signal is a fast pseudoscalar and polarized daughters of the vector ($\rho^0 \rightarrow \pi^+ \pi^-$, $K^{\mp} \rightarrow K^+ \pi^-$); one daughter fast and the other slow. We fully reconstruct the parent B meson and obtain the beam constrained mass (M) and $\Delta E = E - E_{beam}$, both described in Section 3.1. dE/dx and ΔE are used to distinguish between the specific modes. Again, continuum processes dominate the backgrounds. Eleven variables, including energy in cones about the thrust axis, angle between the thrust and the beam axes, the angle between the B meson direction and the beam, and Fox-Wolfram moments, are combined into a Fisher Discriminant to distinguish between continuum and signal. Other backgrounds are reduced by vetoing D^0 's and leptons. The signal yields are extracted by computing unbinned maximum-likelihood fits in the mentioned variables along with the reconstructed ρ^0 or K^{\mp} mass, the angle between the thrust axis of the candidate B and the thrust axis of the rest of the event, and the helicity angle of the vector particle.

Mode	Yield	Efficiency	Branching Fraction
$\rho^0 \pi^{\pm}$	$26.1^{+9.1}_{-8.0}$	$29.6 \pm 2.6\%$	$(1.5 \pm 0.5 \pm 0.4) \times 10^{-5}$
$\rho^0 K^{\pm}$	< 27.5	$27.6 \pm 2.4\%$	$< 2.2 \times 10^{-5}$
$K^{\mp} \pi^{\pm}$	< 21.0	$27.8 \pm 2.4\%$	$< 2.7 \times 10^{-5}$
$K^{\mp} K^{\pm}$	< 6.5	$26.4 \pm 2.4\%$	$< 1.2 \times 10^{-5}$

Table 1. Signal yields from maximum likelihood fits.

The yield contours and example projection plots are shown for the $B^0 \rightarrow h^\pm \rho^0$ fit in Fig. 2. The yields and branching fraction results are shown in Table 1. Data corresponding to 5.8×10^6 $B\bar{B}$ pairs were used for this analysis. For the case of $\rho^0 \pi^\pm$, a significant signal is seen, where first uncertainty in its branching fraction is statistical and the second systematic. This result is the first observed hadronic $b \rightarrow u$ transition. The remaining branching fraction limits are at 90% CL.

5. Summary and Outlook

I presented CLEO's preliminary results on the $b \rightarrow s\gamma$ branching ratio and the CP asymmetry in $b \rightarrow s\gamma$ decays with approximately 3.1 fb^{-1} of on-resonance data, as well as results for a search of B mesons decaying to $h^\pm K^0$ and $h^\pm \rho^0$ with nearly six million $B\bar{B}$ pairs. CLEO has since accumulated a total of 10 fb^{-1} of on-resonance data. Work is underway to determine the $b \rightarrow s\gamma$ inclusive branching fraction and CP asymmetry with all of the data as well as updating limits and branching fractions for the other rare B analyses. We are also exploring extending both $b \rightarrow s\gamma$ analyses by tagging the b flavor with a lepton from the other B meson in the event it undergoes semileptonic decay. This procedure offers further continuum suppression and may improve the asymmetry measurement by allowing the use of events where the b flavor is undeterminable by pseudo-reconstruction.

The installation of the CLEO III detector is currently underway. CLEO III will provide much improved particle identification with a ring imaging Cherenkov detector, which will be extremely useful for the asymmetry measurement and other rare B analyses. Furthermore, we expect to collect approximately 10 fb^{-1} of on-resonance data *per year*. With the improved capabilities of the CESR accelerator and CLEO detector, we expect much more sensitive measurements of $b \rightarrow s\gamma$ and other rare B decays in the next few years.

6. Acknowledgements

The CLEO collaboration gratefully acknowledges the effort of the CESR staff in providing us with excellent luminosity and running conditions. We also thank M. Neubert for bringing the theoretical interest in $b \rightarrow s\gamma$ CP asymmetry to our attention. This work is supported by the National Science Foundation, the U.S. Department of Energy, Research Corporation, the Natural Sciences and Engineering Research Council of Canada, the A.P. Sloan Foundation, the Swiss National Science Foundation, and the Alexander von Humboldt Stiftung.

References

- [1] Y. Gao and F. Würthwein (for CLEO), CALT 68-2220, HUTP-99/A021, hep-ex/9904008 and references therein. For information about $B \rightarrow K\pi, \pi\pi$, and KK also see A. Warburton, these proceedings.
- [2] Y. Kubota *et al.* (CLEO), Nucl. Instrum. Meth. A **320**, 66 (1992).
- [3] M.S. Alam *et al.* (CLEO), Phys. Rev. Lett. **74**, 2885 (1995).
- [4] For example, F. Borzumati and C. Greub, Phys. Rev. D **58**, 74004 (1998); W. de Boer *et al.*, Phys. Lett. B **438**, 281 (1998); H. Baer *et al.*, Phys. Rev. D **58** 15007 (1998). For implications on non-standard model physics see J. Hewett, SLAC-PUB-6521 (1994).
- [5] K. Chetyrkin *et al.*, Phys. Lett. B **400**, 206 (1997); Phys. Lett. B **425**, 414 (1998); A. Kagan and M. Neubert, Eur. Phys. J. C **7**, 5 (1999).
- [6] CLEO conference report 98-17 (ICHEP98 1011).
<http://www.lns.comell.edu/public/CONF/1998/CONF98-17/>
- [7] A. Ali and C. Greub, Phys. Lett. B **259**, 182 (1991).
- [8] J.A. Ernst, Ph.D. thesis, Univ. of Rochester (1995).
- [9] A.L. Kagan and M. Neubert, Phys. Rev. D **58**, 094012 (1998) and M. Aoki, G. Cho, and N. Oshimo, hep-ph/9811251.